Effects of Synthesis Conditions on Macroscopic and Microscopic Properties of Ordered Mesoporous Silica Fibers

Hatem M. Alsyouri and Y. S. Lin*

Department of Chemical Engineering, University of Cincinnati, Cincinnati, Ohio 45221

Received July 23, 2002. Revised Manuscript Received February 3, 2003

Experiments were conducted to prepare ordered mesoporous silica fibers under different conditions (precursor type, temperature, acid concentration, and growth time). The ordered mesoporous silica fibers can be obtained with tetrabutyl orthosilicate as the silica source under the following conditions: temperature at 300 K; and tetrabutyl orthosilicate, cetyltrimethylammonium bromide, HCl, and water molar ratio of 1.0, 0.5, 10−98, and 2000. Synthesis at temperatures above 300 K resulted in ordered mesoporous silica of nonfibrous geometry (films or particles) due to a fast transfer rate of silica source material. A variation in acid concentration in the range of 2.0−6.4 vol % accelerates the formation of fibers with more pore microstructural ordering. Higher acid concentration leads to formation of irregular nonfibrous silica forms besides fibers due to rapid silica hydrolysis/condensation. Under controlled conditions the fibers' diameter becomes larger with a broader distribution for samples with longer growth time. Silica yield increases linearly with growth time. Fibers with different growth times have the same pore microstructure. Fiber length to diameter aspect ratio was in the range 3−30. The experimental results suggest that the fibers grow from the bottom and may coalesce to form fibers with large diameters.

1. Introduction

Discovery of the ordered mesoporous silicates formed by the self-cooperative assembly of inorganic silicate species and organic surfactants is considered a great achievement for the past decade.[1,2] These silicates include a variety of phase structures such as hexagonal (MCM-41) and cubic (MCM-48), and can be prepared in different morphologies including spheres,[3] thin films,[4,5] curved shapes,[6] and rods.[7] These materials have attracted the attention of researchers who hope to elucidate and improve their structures into forms suitable for applications in catalysis,[8] separation,[9,10] optical devices,[11] and controlled polymerization inside their pores.[12−14] MCM-41 is one example of the mesoporous ordered silicates with hexagonally packed, straight, and nonconnected pores of diameter between 1.5 and 10 nm. For applications such as host synthesis of polymer macromolecules, MCM-41 is considered a good candidate because of its uniformly ordered pores. However, its pores are short, falling in the range 100−400 nm.[15] Ordered mesoporous silicates with longer pores are more attractive for a number of applications including the catalyst for production of polymer chains with improved properties unattainable by traditional techniques.

Mesoporous silica fiber (MSF) is another from of ordered mesoporous materials that has a fibrous morphology consisting of hexagonal arrangement of uniformly sized mesopores running along the fiber axis.[16−23] They can be created by the self-assembly of silica source

* Corresponding author. Phone: (513) 556 2769. Fax: (513) 556 3473. E-mail address: jlin@alpha.che.uc.edu.

(1) Kresge, C. T.; Leonowicz, M. E.; Roth, W. J.; Vartuli, J. C.; Beck, J. S. *Nature* **1992**, *359*, 710.
(2) Beck, J. S.; Vartuli, J. C.; Roth, W. J.; Leonowizc, M. E.; Kresge, C. T.; Shmitt, K. D.; Chu, C. T−W.; Olson, D. H.; Shepard, E. W.; McCullen, S. B.; Higgins, J. B.; Schlenker, J. L. *J. Am. Chem. Soc.* **1992**, *114*, 10834.
(3) Grun, M.; Lauer, I.; Unger, K. K. *Adv Mater.* **1997**, *9*, 254.
(4) Yang, H.; Kuperman, A.; Coombs, N.; Mamiche-Afara, S.; Ozin, G. A. *Nature* **1996**, *379*, 703.
(5) Hillihouse, H.; Okubo, T.; van Egmond, J. W.; Tsapatsis, M. *Chem. Mater.* **1997**, *9*, 1505.
(6) Ozin, G. A.; Yang, H.; Sokolov, I.; Coombs, N. *Adv. Mater.* **1997**, *9*, 254.
(7) Schmidt-Winkle, P.; Yang, P.; Margolese, D. I.; Chmelka, B. F.; Stucky, G. D. *Adv. Mater.* **1999**, *11*, 303.
(8) Corma, A. *Chem. Rev.* **1997**, *97*, 2373.
(9) Feng, X.; Fryxell, G. E.; Wang, L. Q.; Kim, A. Y.; Liu, J.; Kemner, K. M. *Science* **1997**, *276*, 923.
(10) Mercier, L.; Pinnavaia, T. J. *Adv. Mater.* **1997**, *9*, 500.
(11) Marlow, F.; Leike, I.; Weidenthaler, C.; Lehmann, C. W.; Wilczok, U. *Adv. Mater.* **2001**, *13*, 307.
(12) Kageyama, K.; Tamazawa, J. I.; Aida, T. *Science* **1999**, *285*, 2113.
(13) Tajima, K.; Aida, T. *Chem. Commun.* **2000**, 2399.
(14) Ye, Z.; Alsyouri, H.; Zhu, S.; Lin, Y. S. *Polymer* **2003**, *44*, 969.
(15) Mokaya, R.; Zhou, W.; Jones, W. *J. Mater. Chem.* **2000**, *10*, 1139.
(16) Huo, Q.; Zhao, D.; Feng, J.; Weston, K.; Buratto, S. K.; Stucky, G. D.; Schacht, S.; Schuth, F. *Adv. Mater.* **1997**, *9*, 974.
(17) Bruinsma, P. J.; Kim, A. Y.; Liu, J.; Baskaran, S. *Chem. Mater.* **1997**, *9*, 2507.
(18) Yang, P.; Zhao, D.; Chmelka, B.; Stucky, G. D. *Chem. Mater.* **1998**, *10*, 2033.
(19) Marlow, F.; Zhao, D.; Stucky, G. D. *Microporous Mesoporous Mater.* **2000**, *39*, 37.
(20) Marlow, F.; Kleitz, F. *Microporous Mesoporous Mater.* **2001**, *671*, 44.
(21) Kleitz, F.; Wilczok, U.; Schuth, F.; Marlow, F. *Phys. Chem. Chem. Phys.* **2001**, *3*, 3486.
(22) Kleitz, F.; Marlow, F.; Stucky, G. D.; Schuth, F. *Chem. Mater.* **2001**, *13*, 3587.
(23) Jung, K. T.; Chu, Y. H.; Haam, S.; Shul, Y. G. J. *J. Non-Cryst. Solids* **2002**, *298*, 193.

10.1021/cm020748b CCC: $25.00
Published on Web 04/12/2003

and organic surfactant by two routes: (a) slow acidic fiber synthesis at oil−water interface at room temperature[16,19−22,24,25] and (b) fiber spinning based on solvent evaporation and sol−gel process.[7,18,23] The slow acidic growth method is simple and can be used to create mesoporous materials of different morphologies and oriented mesoporous thin films at the oil−water interface. The fibers are 100 μm − 5 cm long and have a circular cross-section 1−15 μm in diameter. Fiber spinning method is based on variable-rate hand or machine drawing of fibers from a viscous solution containing the silica source and surfactant. Solution spinnability is based on its viscosity, which is controlled by the sol−gel process or by addition of viscosity enhancement additives such as polymers. Fibers obtained by this method have lengths of 3−10 cm and a diameter of 20−80 μm that can be controlled by the drawing rate.

Microscopy investigations (TEM and optical microscopy) reveal that the pores align parallel to the fiber axis with high fidelity for both synthesis routes. However, some recent studies[11,20,22] show that in the slow acidic synthesis, the pores run in a circular direction around the fiber axis. This observation was based on birefringence and TEM. This novel fiber microstructure was confirmed for several types of silica sources (TEOS, TPOS, and TBOS) and is considered a general property of fibers obtained by the slow acidic route. A mechanism was accordingly proposed to describe this novel architecture. In the proposed mechanism the long rod surfactant micelles available in the synthesis media undergo aggregation and restructuring processes that lead to formation of nanoscopic coil seeds. The simultaneous growth of seed coils by further aggregation of long rod micelles around the coils and silica condensation around the coil seeds causes the formation of the inner circular architecture from hexagonally packed pores. In the fiber spinning method, which is essentially a mechanical action, the solvent evaporation controls the micrometer scale morphology. During solvent evaporation after fiber spinning, silica and surfactant self-assemble to form the hexagonal mesophase structure.[17,18,23]

Although the spinning method has some application-related advantages over the slow acidic method, including obtaining longer fibers, the nature of acid fiber synthesis offers better prospects for studying the fiber formation process and its properties due to its simplicity and flexibility to be used over a wide range of variables. Several studies have utilized the slow acidic synthesis to prepare MSF under various conditions of silica precursors, solvents, and acid concentrations.[16,22] Most of these studies have focused on exploring the microscopic properties and formation of the internal structure of the fibers. Little attention was given to the effect of the synthesis conditions such as acid concentration and growth time on the fiber kinetics and the macroscopic properties such as fiber diameter and length, which are key factors for some applications. In the present work, MSF was prepared under different synthesis conditions of precursor type, growth times, acid concentrations, and temperatures. The influence of synthesis conditions on MSF macroscopic properties such as yield, fiber length, and diameter, and their distributions, was investigated. The macroscopic results will also give some insight into the mechanism of formation of fiber and particulate morphologies.

2. Experimental Section

2.1 Synthesis. Mesoporous silica fiber samples were prepared using cetyltrimethylammonium bromide (CTAB) (Aldrich) as surfactant and tetrabutyl orthosilicate (TBOS) (Aldrich) as silica source in acidic synthesis based on procedures described in the literature.[16,20] Three sets of MSF samples were prepared under three different variables: growth time, acid concentration, and temperature. The standard preparation conditions were 1:0.5:58.4:2000 TBOS/CTAB/HCl/H_2O molar ratio at room temperature and aged for 7 days. For MSF preparation at different growth times the samples were aged for 4, 7, and 10 days with molar ratio and temperature conditions similar to those of the standard. Different acid concentration samples were prepared with HCl/TBOS molar ratios ranging from 4 to 148. Nine samples were accordingly prepared with HCl volume percentage of 0.4−12% with other conditions the same as the standard conditions. Finally, samples at different temperatures were prepared at 300, 323, and 338 K under the same conditions.

In the synthesis, CTAB was dissolved in water under mild mixing. Subsequently, HCl (6 M) was added slowly and the solution was mixed until it became clear. This solution (H_2O, CTAB, and HCl) is referred to as the water phase. Mixing was stopped and TBOS (referred to as silica phase) was slowly added to form a thin layer above the aqueous solution. After almost 2 days a thin film was observed at the interface between the water and silica phases. Silica fiber started to grow from the bottom of the thin film toward the water phase approximately after 2−3 days. After aging for the required growth time, silica fibers were removed carefully, washed with deionized water, and dried in air. Calcination was carried out at 813 K for 6 h to remove the surfactant. MSF synthesis was also attempted by using a mixture of tetraethylorthosilica (TEOS) (Aldrich) with organic solvent (hexane) as the silica phase.

2.2 Characterization. Powder X-ray diffraction (XRD) patterns were obtained on a Siemens D-50 using CuKα radiation. XRD spectra were taken between 2θ of 1.5−8 and used to identify the phase structure and interplaner (d) spacings. Nitrogen adsorption−desorption measurements were performed on a Micromeritics ASAP-2000. The samples were degassed at 473 K for 2 h and analyzed at 77 K. The adsorption isotherm was used to calculate the BET surface area and pore volume. The desorption isotherm was used to obtain the pore size distribution, from which the average diameter was calculated. Morphology and fiber diameter and length distributions were studied by scanning electron microscopy (Cambridge S-90B) and light microscopy (Optiphot100 Nikkon). The fiber diameter and length distributions and aspect ratio were estimated by taking a representative section from the fiber microscope image and measuring the diameter and length of 100 randomly selected fibers. From the measured values the fiber length and diameter accumulative curves were constructed. The fiber diameter and length distributions can be calculated from the cumulative curves by taking slopes at different points.

The silica yield is defined as the mass ratio of the MSF formed to the total mass of silica present in the TBOS input. It is calculated using the calcined MSF weight, TBOS mass input, and the theoretical silica (SiO_2) production per gram of TBOS input which is 0.2 g/1 g SiO_2/TBOS (yield = calcined MSF mass/TBOS mass × 0.2). The consumption of the surfactant (CTAB) was calculated from the difference in MSF weight before and after calcination. The yield and consumption of the surfactant values indicate the amounts of TBOS and surfactant, respectively, utilized to produce MSF.

(24) Huo, Q.; Feng, J.; Schuth, F.; Stucky, G. D. *Chem. Mater.* **1997**, *9*, 14.
(25) Schacht, S.; Huo, Q.; Voigt-Martin, I. G.; Stucky, G. D. *Science* **1996**, *273*, 768.

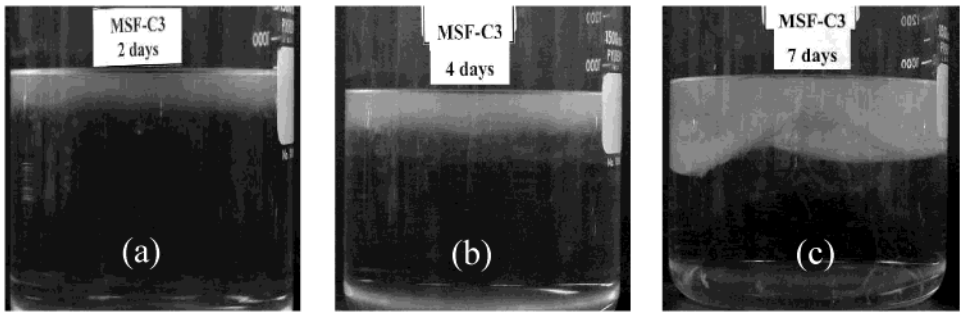

Figure 1. Fiber growth for MSF sample prepared with 8.4 vol % HCl at 300 K (HCl/Si molar ratio of 98): (a) after 2 days; (b) after 4 days; and (3) after 7 days.

3. Results and Discussion

3.1 Results of Synthesis. In the acidic, stagnant synthesis media, the silica source diffuses slowly through the silica−water interface to the water phase and condenses with the surfactant micelles to form three different silica forms: amorphous thin film or membrane at the silica-water interface; silica fibers grown from the bottom of the thin film in the water phase; and small fine particles that usually precipitate in the bottom of the water phase. The amount of each form and the fiber growth rate are dependent on the precursor type and growth conditions. Samples prepared at different growth times show that after 2 days the thin film started to grow at the interface between the silica and water phases in addition to some traces of fibers appearing in the water phase with its base attaching to the bottom of the thin film. After 4 days of growth a white complicated network of interwoven fibers can be seen in the water phase. Typical appearance of the MSF growth for the three different growth times for a sample prepared with 8.4 vol % HCl is shown in Figure 1. Some of the fibers grow longitudinally with maximum length exceeding 5 cm.

Fine particles can be observed almost from the third day of growth. When fine particles start to precipitate their amount relative to that of the fibers is small. In general the amount of the three different forms increases with growth time. However, growth of the fiber form is the most significant. The amount of fibers increases almost linearly with time under the studied range of growth times. The ratios of fibers to fine particles and to the film become larger as growth time proceeds from 4 to 10 days.

The source of silica used can affect the form of the silica grown during synthesis. For example, growth using a TEOS silica source, dissolved in hexane using the above-given molar ratio, led to the formation of only a relatively thick amorphous film without any fibers or particles. Other molar ratios of TEOS can produce fibers as demonstrated by other studies.[16,22] On the other hand, when TBOS was used, a thin film, fibers, and fine particles were formed during synthesis with the fiber amount relatively larger than that of the fine particles. For this reason TBOS was used as the silica source to study the effect of other growth conditions on the type, composition, and properties of the silica forms.

MSF preparation under different HCl acid concentrations led to the three different forms of silica with relatively small amounts of finer particles. In general, three growth trends have been observed for MSF synthesis for 7 days under various acid concentrations: (1) no growth of any silica form at acid contents ≤0.4 or ≥12% vol %; (2) slow fiber growth at 1.0−2.0 vol % and 8.4−12.0 vol % acid; and (3) fast fiber growth at 2.0−8.4 vol % range of acid content. In the fast growth range, fibers start to grow earlier, as compared to the slow growth range where fiber growth becomes very slow and may take a long time (few weeks) to form. This behavior gives a maximum in the fiber amount at 6.4 vol % HCl concentration. At concentrations lower than 0.4 or higher than 12.0 vol % no fibers were formed within 7 days of growth. Growth at high acid concentration may produce only a thick film at the silica−water interface.

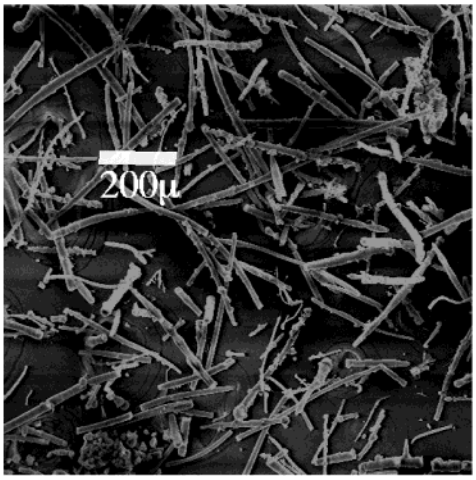

Figure 2. SEM image of sample grown for 10 days showing the fiber morphology. Sample was prepared at 300 K with 5.1vol % acid (HCl/Si molar ratio 58).

Preparation of fibers at high temperatures (323, 338 K) did not show the production of any fibers. The synthesis ended up with only particles grown at the interface and in the bulk of the water phase. The particles have hexagonally ordered mesoporous pores typical of MCM-41. This behavior at high temperature could be attributed to two factors: enhanced diffusivity of silica source in the water phase, and the presence of convection streamlines inside the water phase. These factors can act together to supply silica source to the surfactant micelles from 3 directions both at the interface and inside the water phase. This 3-dimensional growth causes the formation of particle morphology rather than fibrous morphology.

3.2 Macroscopic Properties. Figure 2 shows a macroscopic view of the silica fibers. The diameter of the fiber, as shown in Figure 3, is around 10 μm. The

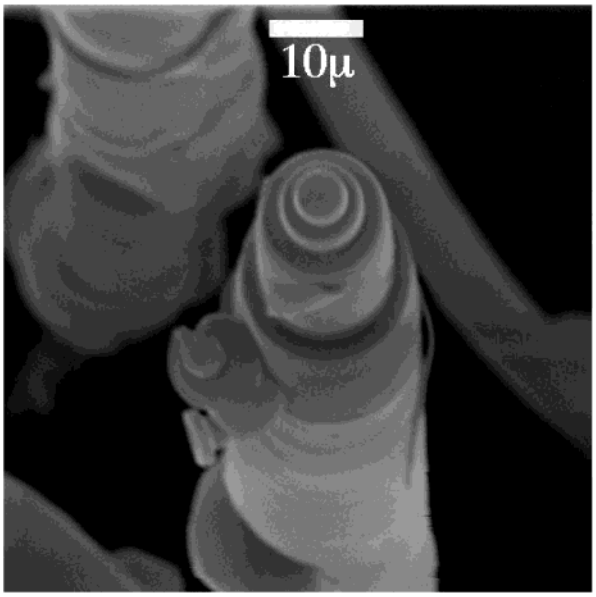

Figure 3. Enlarged view of cross-section of a mesoporous silica fiber (prepared under the same conditions as that in Figure 2).

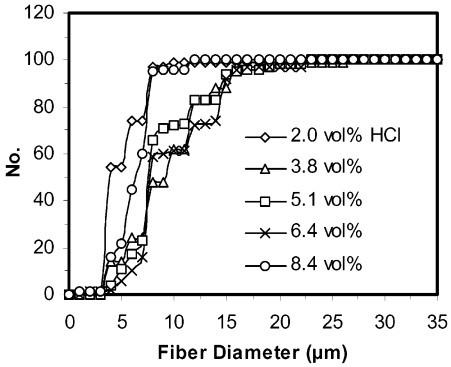

Figure 4. Accumulative fiber diameter distributions curves at different acid concentrations.

fibers observed under microscope appear to be uniform in length, about 200−300 μm, which, however, does not represent the original length of the fibers of up to a few centimeters. The process of collecting fibers from the synthesis solution caused breakage of the fibers along the length direction (not diameter). Therefore, the diameters of the fibers observed under the microscope could be a close approximate of the fibers in the synthesis solution. Diameter distributions for the prepared silica fibers were estimated from the micrographs. Figure 4 shows fiber diameter distribution for the samples prepared with different acid concentrations. The results of the fiber sizes and silica yields for these samples are summarized in Table 1. As shown, the fiber diameters increase with acid concentration reaching a maximum at 6.4 vol % and then start to decrease at higher concentrations. The acid concentration of 6.4 vol % (corresponding to HCl/Si molar ratio of 73) gives the silica fiber with largest average diameter and broadest fiber diameter distribution and highest silica yield. The surfactant consumption rate and silica yield show behavior similar to that of the fiber diameter with increasing acid concentration. The highest silica yield and surfactant consumption occur at 5.0−6.4 HCl vol %.

Table 1. Fiber Diameter, Mass Production, and Yield of Mesoporous Silica Fibers Prepared at Different Acid Concentrations (T = 300 K, growth time = 7days)

HCl vol %	fiber diameter (μm)		% silica yield	% CTAB consumption
	average	distribution		
2.0	6	4−12	5.62	0.98
3.8	9	4−18	6.81	5.60
5.1	9	4−18	19.94	9.62
6.4	10	4−24	20.71	6.47
8.4	7	4−12	8.64	0.78

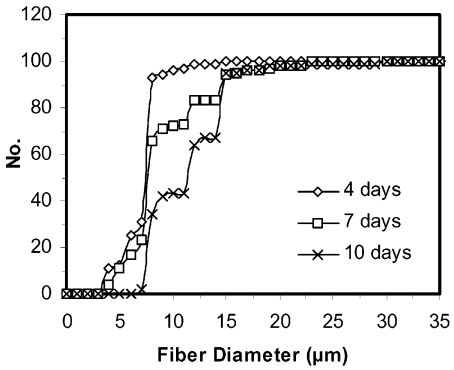

Figure 5. Accumulative fiber diameter distributions curves at different growth times.

Table 2. Fiber Diameter, Mass Production, and Yield of Mesoporous Silica Fibers Prepared with Different Growth Times (T = 300 K at 5.1 Vol % HCl)

growth time (day)	fiber diameter (μm)		% silica yield	% CTAB consumption
	average	distribution		
4	6	3−11	7.65	2.08
7	9	4−18	19.94	9.62
10	12	7−22	34.69	16.89

Figure 5 shows the accumulative fiber distribution for samples prepared under different growth times. The average fiber diameter and diameter range for the samples with three different growth times are summarized in Table 2. As shown in Figure 5, the average fiber diameters are, respectively, about 6, 9, and 12 for samples with growth times of 4, 7, and 10 days. The distribution of fiber diameter becomes broader as growth time increases. The silica yield and surfactant consumption of fibers prepared with different growth times are also summarized in Table 2. As shown, the low values of yield and CTAB consumption for production of MSF reflect that the formation process is slow and encounters high resistance. Main resistances include resistance to silica source diffusion from the strong hydrophobic silica phase to the hydrophilic water phase through the film at the interface, and resistance to silica diffusion to the aggregated surfactant inside the water phase. The surfactant may face some resistance to diffusion toward the silica source inside the water phase, but it is, in general, small because mixing of the water phase before adding the silica source causes the surfactant to be well distributed and available in the molecular scale.

Figure 6 plots fiber yield versus growth time. The first 2 days appear to be the induction period during which no fiber is formed. It is interesting to note that fiber mass production is linearly dependent on the growth time as shown in Figure 6. Silica source mass transfer and MSF mass production are inversely proportional to the diffused length inside the water phase, i.e., $M_{MSF} = A \times D_{SW} (\Delta C/L)t$ where M_{MSF} is the fiber mass produc-

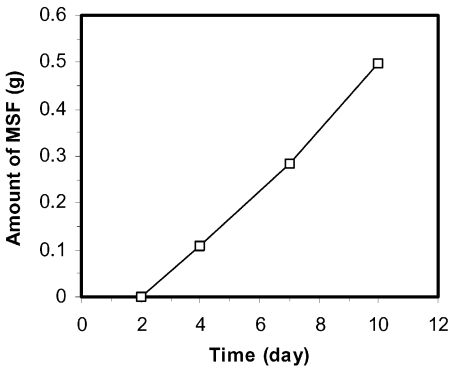

Figure 6. Effect of aging time on mesoporous silica fiber mass production for samples prepared at 300 K with 5.1 vol % acid (HCl/Si molar ratio 58) for 4−10 days.

tion, A is the diffusing area, D_{SW} is the diffusion coefficient for silica source in the water phase, ΔC is the concentration difference of silica source between the silica and water phase, L is the diffusion length, and t is the growth time. Silica fibers grow in length with time (L is increasing) and their heads go deep in the water phase. If the silica fibers are assumed to grow from their heads this implies that the silica source must diffuse a long distance, L, to condense at the silica head so the fiber mass production rate should decrease with the growth time. However, the linear dependency of fiber mass production with time may indirectly imply that the fibers grow from their bottoms rather than their heads.

The average fiber diameter increases from 6 to 12 μm when the growth time increases from 4 to 10 days. If one assumes the increase in the silica yield is due to increase in the fiber diameter, with the fiber length and fiber number remaining constant, then the silica yield should be proportional to squares of the fiber diameter. The experimental data listed in Table 2 appear to follow this relationship. However, we clearly observed that fiber length increases substantially with the growth time, as indirectly shown in Figure 1. It is more likely that the increase in the silica yield is due to growth of the fiber in the length direction, not the diameter. It is possible that with increasing growth time fibers coalesce to form large fibers, thus decreasing the total number of fibers present in the synthesis vessels.

Fiber aspect ratio, defined as fiber length-to-diameter ratio, was estimated from micrograph images. It was found that the aspect ratio for MSF samples prepared under both aging time and acid concentration variables lies in the range of 3−30 with average value close to 12. Very few fibers (<5%) show an aspect ratio larger than 50. These values correspond to broken fibers as a result of the sample collection process. Fibers with original length could have aspect ratio values of at least 5000.

3.3 Microscopic Properties. Figure 7 shows the XRD patterns for three samples prepared at different growth times. The samples show the presence of three reflection peaks indexed as (100), (200), and (110) planes and a lattice parameter a = 3.9 nm. The peaks are indexed as (hk0) and indicate the presence of long-range order of hexagonally arranged long pores inside the fiber. It can be noticed that longer growth time not only results in longer and bigger fibers but also improves the

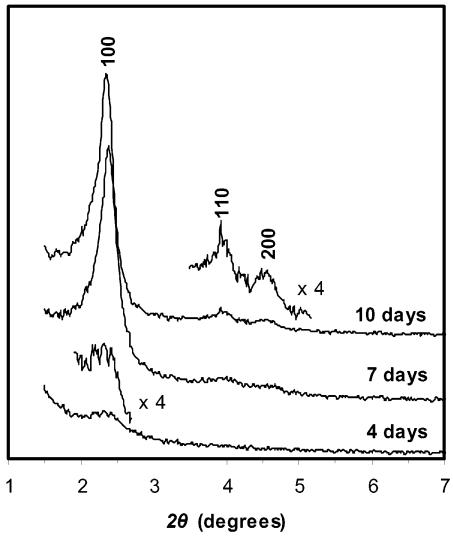

Figure 7. XRD patterns for samples under different growth times.

Table 3. Interplanar Spacing and Pore Wall Thickness, and N_2 Adsorption−Desorption Results for the Samples Prepared at Different Growth Times (T = 300 K at 5.1 Vol % HCl)

growth time (day)	interplanar spacing d_{100} (nm)	BJH pore size (nm)	pore wall thickness (nm)	pore volume (m^3/g)	BET surface area (m^2/g)
4	3.90	2.5	1.4	0.32	610
7	3.71	2.48	1.23	0.59	1032
10	3.77	2.42	1.35	0.72	1107

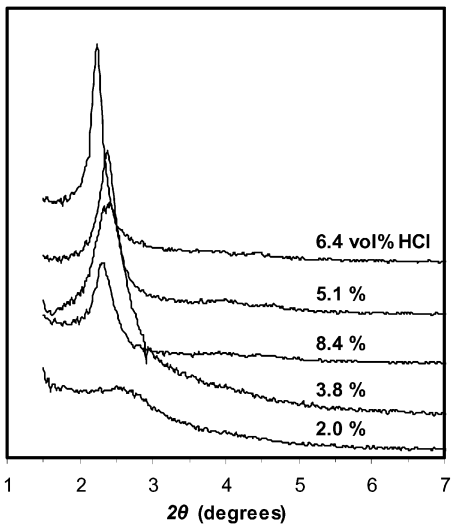

Figure 8. XRD patterns for samples under different acid concentrations.

uniformity of the fiber hexagonal pore structure as indicated by increasing the intensity and the number of XRD peaks in Figure 7. The pore structures of the silica fibers with different growth times are summarized in Table 3. Within the accuracy of the data, the interplanar spacing, pore size, and pore wall thickness of all three silica samples are similar. All samples under different aging times are mesoporous with average pore diameter of ca. 2.5 nm. However, the surface area and pore volume increase with increasing growth time.

Figure 8 shows the XRD patterns for samples prepared at different acid concentrations. All samples, except at 2.0 vol %, exhibit clear XRD peaks indicative

Table 4. Interplanar Spacing and Pore Wall Thickness, and N_2 Adsorption−Desorption Results for the Samples Prepared at Different Acid Concentrations (T = 300 K, growth time = 7 days)

HCl vol %	interplanar spacing d_{100} (nm)	BJH pore size (nm)	pore wall thickness (nm)	pore volume (m^3/g)	BET surface area (m^2/g)
2.0	3.5	2.52	0.98	0.44	865
3.8	3.69	2.48	1.21	0.74	1525
5.1	3.71	2.48	1.23	0.59	1032
6.4	3.94	2.40	1.54	0.35	812
8.4	3.81	2.31	1.50	0.49	906

of ordered mesopore structure. In the case of low acid content, 2.0 vol %, a low signal-to-noise ratio suggests the presence of amorphous product. The increase in acid content is accompanied by a narrow and higher intensity (100) peak indicating a substantial improvement in structural ordering. The best quality hexagonal structure was observed for the sample obtained with 6.4 vol %. Further increase in the acid concentration, ≥8.4%, leads to reduction in pore ordering as indicated by reduction in the pore intensity. The pore structures of these samples are summarized in Table 4. As shown, increasing acid concentration causes slight increase in the interplanar spacing, d(100), between 3.5 and 3.94 nm. The change in interplanar d(100) spacing can be caused by a change in pore wall thickness (w_p) and /or pore size (d_p) since $d(100) = w_p + d_p$. As shown in Table 4, increasing acid content causes a very slight decrease in the pore size (∼1 Å) compared to ∼2−3 Å increase in pore wall. Therefore, the net effect of acid content increase on increasing the d(100) is due to the increase in the pore wall thickness at relatively constant pore size. Change in surface area and pore volume was not uniform and can be sensitively affected by the presence of some amorphous particles in the fiber sample.

Acid is usually added to the synthesis mixture as a catalyst for silica hydrolysis and condensation. The increase in the pore wall thickness with increasing acid content is due to formation of more silica framework possibly due to enhanced hydrolysis and condensation of TBOS in the presence of a larger amount of acid. Acid can also affect the aggregation of surfactant rod micelles through a reduction in the surfactant molecules head area by means of re-distribution of charge at the surfactant molecule head and causes the rod micelle diameter to become smaller.[26] This could cause the slight decrease of the pore size with increasing acid content. Nonuniformity in surface area and pore volume properties could be attributed to the presence of some denser, nonfiber particles collected together with the silica fiber sample. As described earlier, the silica fiber growth is accompanied by the formation of amorphous thin film and fine particles. In the bottom-left and upper-right corners of the SEM images in Figure 2 such silica particles can be seen. Several samples of nonfibrous silica forms (e.g., thin film) were carefully collected from the synthesis beakers prepared at different growth times and acid concentrations and tested by XRD and N_2 adsorption. These samples exhibit an amorphous XRD pattern without reflection peaks and have smaller surface areas (about 145 m^2/g) and pore volumes (0.20 cm^3/g). These amorphous silica particles are possibly formed by hydrolysis and condensation of silica source without involvement of the template.

(26) Sprokel, G. J. *The Physics and Chemistry of Liquid Crystal Devices*; Plenum Press: New York, 1980.

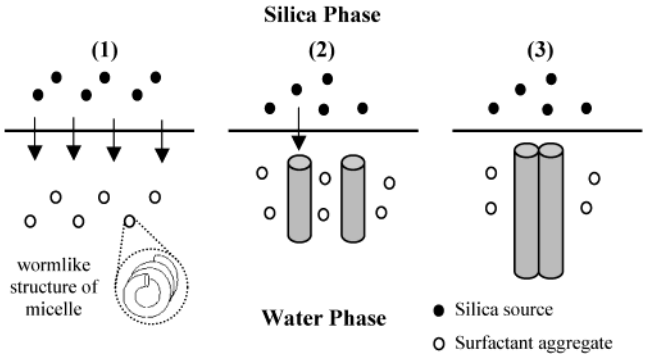

Figure 9. Schematic description of the mechanism of fiber formation: (1) slow diffusion of silica source through the interface toward the aggregated surfactant; (2) growth of silica fiber from the base rather than the heads; and (3) aggregation of two neighboring fibers to form one larger-diameter fiber.

The silica fibers grow longer with the growth time. Therefore, the portion of the silica fibers with larger surface area and pore volume in the sample collected increases with the growth time. Thus, the samples with longer growth time exhibit higher surface area and large pore volume per unit gram of the sample including both ordered mesoporous silica fiber and denser silica particles. Acid concentration may also affect the relative quantity of the denser silica particles contained in the samples collected by affecting the rate of hydrolysis and condensation of silica source in the presence of template. If the rate of hydrolysis and condensation of silica is balanced by the presence of flexible template, well-developed macroscopic fibers will be formed.[22] At higher acid content, silica formation becomes rapid and may proceed to form nonfibrous irregular forms besides the ordered fibers. This can reduce the overall uniformity of the sample as apparent for the sample with 8.4 vol % acid which has less resolved diffraction pattern (Figure 8) and microstructural properties (Table 4). Thus, the nonuniformity of different pore volumes and surface areas of the samples under different acid contents could be due to different percentages of the denser particles in the samples.

3.4 Mechanism of Formation. Early studies about mesoporous silica fibers[16] assumed that MSF has hexagonally packed pores that lie straight across the fiber length. However, it was found later[11,22,26] that fibers have hexagonal pores running in a circular direction about the fiber axis and a mechanism of formation was accordingly suggested to explain the formation of this microscopic structure. These later studies did not highlight the importance of the macroscopic properties which may provide some useful insight into the fiber morphology formation mechanism. Here we propose a simple mechanism, schematically shown in Figure 9, based on the results obtained in this study.

As illustrated in Figure 9, the synthesis vessel at the beginning consists of a hydrophilic water phase containing a stable solution of cylindrical micelles. After the addition of silica phase, TBOS starts to diffuse to the water phase. Because the silica phase is strongly hydrophobic it will diffuse very slowly in a one directional fashion. At the silica−water interface region

where the amount of surfactant is small relative to the body of the water phase, diffused TBOS will undergo hydrolysis and condensation without involvement of the surfactant. This will result in formation of an amorphous film at the interface, through which TBOS will continue to diffuse into the water phase. The cylindrical micelles can undergo restructuring and aggregation processes under the effect of dissolved silica species by means of van der Walls attraction, leading to the formation of long, wormlike micelles.[20,27] The wormlike micelles will then undergo more restructuring and aggregation processes to form the internal structure with rods running circularly across the aggregate axis.[26]

Large amounts of the long aggregated rod micelles will be available at the interface and will start to self-assemble with the uni-directionally diffused silica to form fibers with their structure controlled by aggregation of the wormlike micelles. The wormlike micelles will be, somehow, continuously supplied at the base of the fiber and condense with the incoming diffused silica to grow the fiber from its bottom. From here it is clear why the percentage of silica source consumption is higher than the surfactant consumption. This is most probably due to the high resistance encountered by the surfactant micelles diffusing in the water phase toward the base of the fiber. At the early stages of fiber growth most of the grown fibers are small in diameter and length. The presence of some wormlike micelle aggregate between two small neighboring fibers could lead to combining these two fibers by means of silica condensation with the micelle, and the unsaturated silica groups at the surface of the other fibers ending up with a fiber with larger diameter. If the diffused silica source was not accompanied by the presence of flexible aggregated micelles, the silica hydrolysis/condense reactions will proceed without involvement of micelle and thus produce amorphous particles. These simultaneous processes continue and lead to the observed macroscopic properties.

(27) Atkins, P. W. *Physical Chemistry*; Oxford University Press: New York, 1994.

4. Conclusions

Synthesis of ordered mesoporous silica fibers is very sensitive to the synthesis conditions. Ordered mesoporous silica fibers can be obtained with TBOS as the silica source under a narrow range of experimental conditions (temperature at 300 K; and TBOS/CTAB/HCl/H_2O molar ratio of 1:0.5:10−98:2000). Amorphous silica films or particles are formed with TEOS as the silica source dissolved in hexane. Ordered mesoporous silica of nonfibrous geometry (films or particles) can be obtained at higher synthesis temperatures (above 300 K). The increase in acid concentration speeds up the formation of silica and may produce amorphous nonfibrous particles besides the ordered fibers. Under controlled conditions the fibers diameter becomes larger with a broader distribution for samples with longer growth time. Silica yield increases linearly with growth time. Fibers with different growth times have the same pore microstructure. The experimental results suggest that the fibers grow from the bottom and coalesce to form larger fibers.

Acknowledgment. The project was supported by the NSF through grant CTS-008076.

CM020748B